Macromolecules

Volume 39, Number 12 June 13, 2006

Communications to the Editor

Nanoporous Polyethylene Film Prepared from Bicontinuous Crystalline/Amorphous Structure of Block Copolymer Precursor

Hiroki Uehara,*,† Tomoyuki Yoshida,† Masaki Kakiage,† Takeshi Yamanobe,† Tadashi Komoto,† Kumiko Nomura,‡ Katsuhiko Nakajima,‡ and Masatoshi Matsuda‡

Department of Chemistry, Gunma University, Kiryu, Gunma 376-8515, Japan, and Material Engineering Division, Toyota Motor Corp., Toyota, Aichi 471-8572, Japan

Received January 19, 2006
Revised Manuscript Received April 12, 2006

Block copolymer is capable of organizing various self-assembly structures on a nanometer scale. This unique characteristic has been utilized for preparation of the materials composed of nanometer pores.[1−11] However, such an application of block copolymer is often limited to ultrathin films. Its restricted longitudinal space induces the periodic arrangement of the phase separations, which spreads over a lateral direction parallel to the surface.[1,3,7,8,11] In this work, we demonstrate an easy method of preparing a nanoporous polyethylene film having submillimeter thickness from a block copolymer precursor.

The block copolymer exhibits various types of microphase separations, including spherical, cylindrical, and lamellar structures, depending on the component ratio of the different blocks. Among these morphologies, the sphere is most widely used as a precursor of nanoporous materials. Recently, Yokoyama et al.[9] developed a pore preparation method with supercritical CO_2, which remains in the spheres and expands, giving numerous nanopores within the sample. A cylinder can also be converted to the continuous pore structure when it can be removed. Hillmyer et al.[4,5,10] prepared nanoporous materials from polystyrene (PS)/poly(lactic acid) (PLA), poly(cyclohexyl ethylene)/PLA, or PS/poly(ethylene oxide) (PEO) diblock copolymers by selective removal of PLA or PEO cylinders using alkali or acid solvents. Here, an orientation of the original cylinders perpendicular to the etched surface is required to improve the resultant pore continuity. Therefore, an extrusion technique with a channel die was used.

In contrast, a lamellar structure is not used for preparing nanoporous material, but the gyroid structure,[12] which is one type of diagonals between lamella and cylinder, is used. This structure is composed of a set of two networks having different chemical structures. Selective removal of one network produces the continuous nanopores without any additional processing. Thomas et al.[2] successfully prepared nanoporous ceramic films from triblock copolymer precursors having the double-gyroid structure. A combination of ozonolysis and ultraviolet irradiation causes the selective removal of the hydrocarbon block and the conversion of the silicon-containing block to a ceramic structure. The calculated interfacial area of this nanoporous ceramic film approached 40 m^2/g due to the unique gyroid interconnections of both blocks within the precursor.

These phase separations of block copolymer are dominated by the component ratios of the precursor blocks, which are determined by the chemical synthesis of the starting material. In contrast, we tried to control the phase separation by inducing another self-assembly ability of "crystallization" in the blocks. If one or more blocks are semicrystalline, the two self-assembly effects of the usual phase separation induced by chemical difference and crystalline/amorphous separation will overlap. This suggests the possibility that the phase separation of block copolymer is controllable by crystallization procedure without any chemical change.

Usually, the amorphous phase is more easily etched than the crystalline phase by chemicals or irradiations. Thus, the selective removal of the amorphous phase leaves the remaining networks composed of the crystalline phase alone. Its higher mechanical properties, compared to those of the amorphous phase, restrict the collapse of the resultant nanoporous structure even if it has a large empty space within the free-standing films. This is a significant advantage for the postapplication of these nanoporous materials, as, for example, the filtration membrane or battery

† Gunma University.
‡ Toyota Motor Corp.
* Corresponding author. E-mail: uehara@chem.gunma-u.ac.jp.

10.1021/ma0601316 CCC: $33.50
Published on Web 05/13/2006

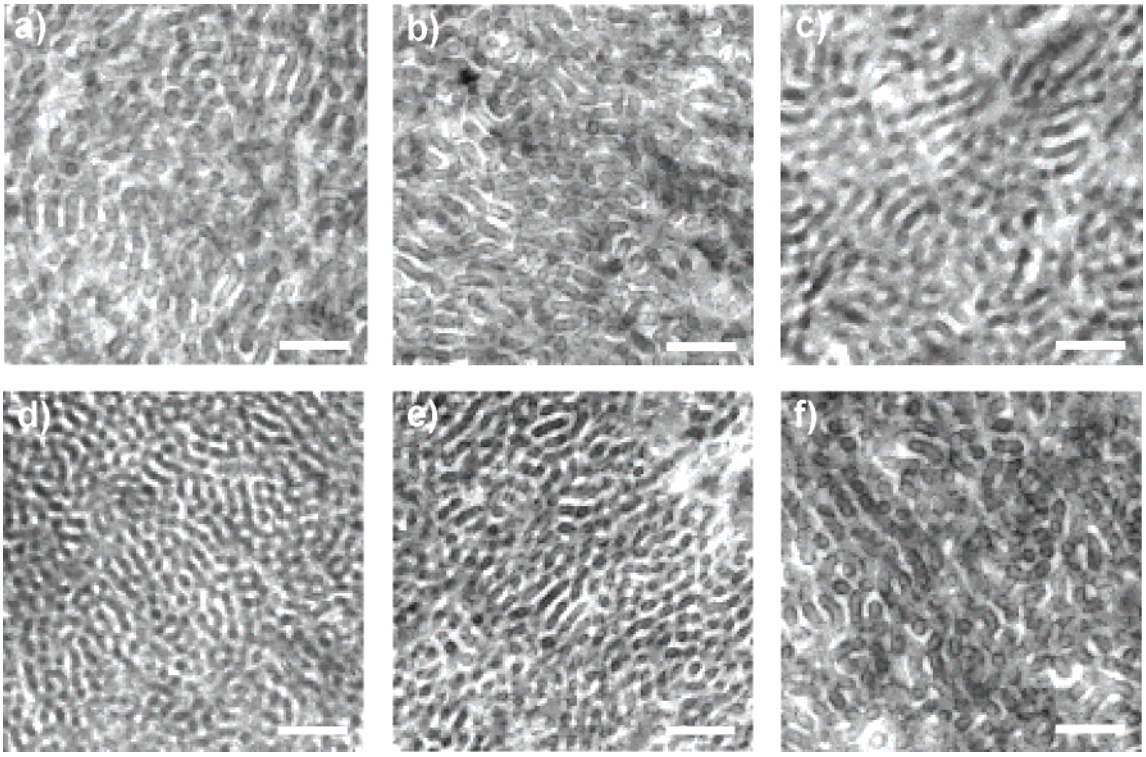

Figure 1. A series of TEM images of the PS-*b*-PE films isothermally crystallized at different T_c's for 24 h: (a) 70, (b) 75, (c) 80, (d) 85, (e) 90, and (f) 95 °C. All scale bars are 250 nm. The films were stained by RuO_4, followed by ultra-microtomed into 60 nm thick. Bright and dark regions correspond to PE crystalline phase and amorphous phases containing PS component.

separator. The resistance to the high loading force is required for high-speed filtration at the high pressure. Similarly, roll-processing of the lithium ion battery cell should employ separator materials with high mechanical performance to achieve higher density fabrication. Both of these applications are possible due to the flexibility of the materials, which ceramics lack.

Therefore, we chose polyethylene (PE)/PS diblock copolymer as our starting material. The number-average molecular weight (MW) of each component was 5.4×10^4 for PS and 6.7×10^4 for PE, with a MW distribution of 1.04. The PE block is semicrystalline, but the PS block is always amorphous. Thus, their crystalline/amorphous phase separations were controlled by processing conditions, including isothermal crystallization temperature and time after the melt. The details of the experimental procedures are described in the Supporting Information. The prepared sample film was melted at 180 °C and then isothermally recrystallized at various temperatures (T_c) for 24 h in a differential scanning calorimetry (DSC) cell under nitrogen gas flow. Figure 1 shows a series of transmission electron microscope (TEM) images of the PS-*b*-PE films isothermally crystallized at T_c's of 70−90 °C. At the lower T_c, the bright regions corresponding to PE crystalline phases are less pronounced and discontinuous but gradually grow and connect each other by increasing crystallization temperature, resulting in the greatest crystallization at an optimum crystallization of $T_c = 90$ °C. However, the further higher T_c of 95 °C again gave the discontinuous morphology of the PE crystalline phases, similar to that obtained at the lower T_c of 70 °C. Since the effective crystallization could not be achieved at such higher T_c, thus the isothermal crystallization procedure has the same meaning as the hindered crystallization on direct quenching from the molten state.

As compared to these TEM images for the films crystallized at the lower and higher T_c's, the periodicity of the crystalline phases is quite different. The packing of the crystalline phases becomes congested with increasing the effective T_c. This implies that the crystallization proceeds with the further phase separation into the crystalline and amorphous regions within the PE component.

For further application of this characteristic crystalline/amorphous morphology as a bulk material, the larger sized film, having a radius of 90 mm and a thickness of 30 μm, was prepared by the same solution-casting method. The obtained film was melted at 180 °C and then isothermally crystallized at an optimum $T_c = 90$ °C in a vacuum oven for 3 days. The internal structure was analyzed with a grazing angle by scanning electron microscopy (SEM). As illustrated in Figure 2a,b, the resultant crystalline/amorphous phase separation exhibited the preferable bicontinuous network structure, where crystalline and amorphous cylinders are interconnected. The diameters of both crystalline and amorphous network cylinders are about 30 nm. The crysallinity of PE component, as estimated by density measurement, was 45%.

If only the amorphous component could be decomposed from such a bicontinuous network structure, the remaining crystalline network would be a material having continuous nanometer-sized pores passing throughout the film thickness. Considering the complicated network geometry of bicontinuous crystalline/amorphous phase separation, we applied a fuming nitric acid etching to this film. Fuming nitric acid etching is often used to selectively remove the amorphous phase of PE.[13−17] Its liquid state enables easy penetration into the film at submillimeter depths from the surface. Therefore, this etching method is desirable for preparing nanoporous structured bulk. In this study, a fuming nitric acid etching was performed at room temperature at times ranging from 1 min to 1 h, followed by washing and drying. With increased etching time, the pores gradually developed and interconnected with each other. However, the 1 h etching destroyed the crystalline networks, and the pores collapsed. The largest pore size and most developed intercon-

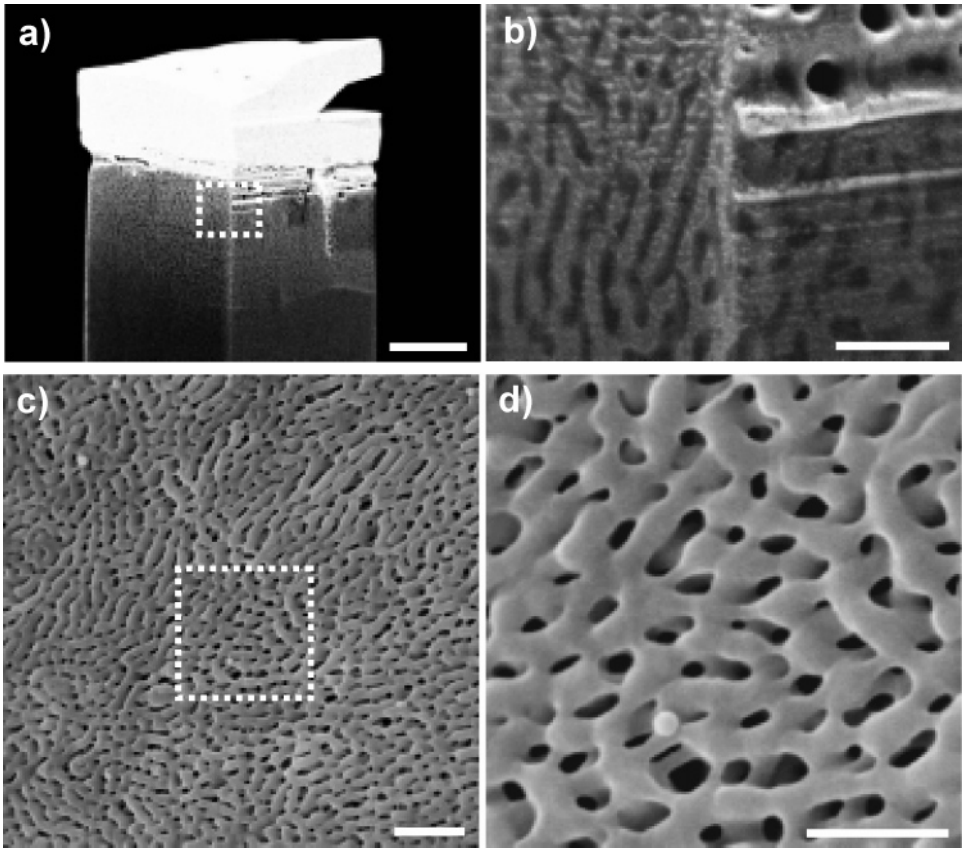

Figure 2. Comparison of initial morphology of the film isothermally crystallized at 90 °C (a and b) and crystalline network morphology obtained after acid etching (c and d). (a**)** Grazing SEM image with a scale bar of 1 μm. The square pole was cut from the film by an focused gallium ion beam procedure in the SEM chamber. Bright and dark regions within the internal structure correspond to the PE crystalline phase and amorphous phases containing PS component. (b**)** Enlarged image of the area marked by the dotted line in (a**)** with a scale bar of 200 nm. (c**)** Usual SEM image with a scale bar of 1 μm. (d**)** Enlarged image of the area marked by the dotted line in (c**)** with a scale bar of 200 nm.

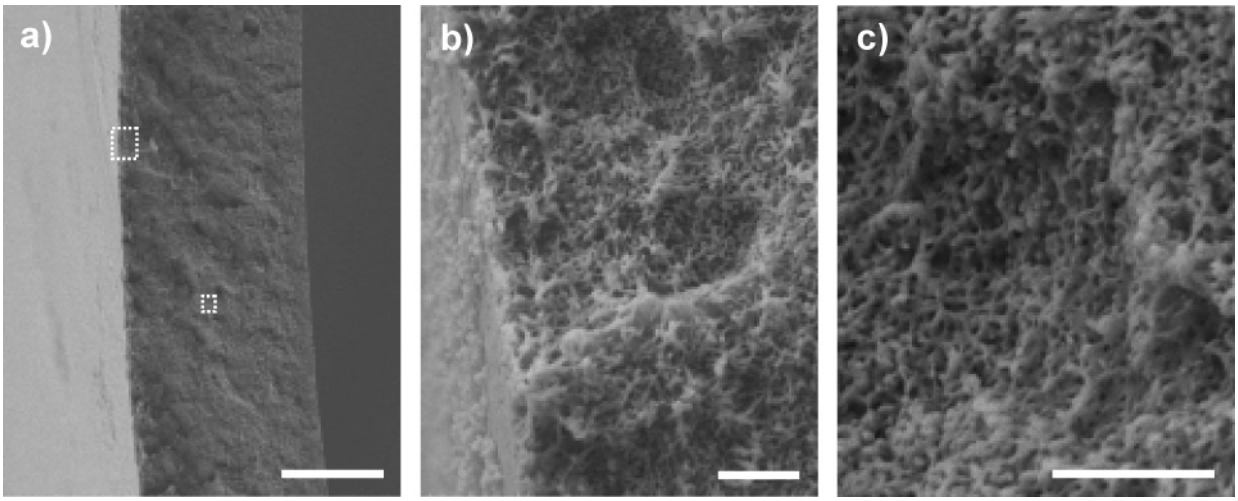

Figure 3. SEM images of the edge of the film etched for 30 min. The film was freshly cleft in liquid nitrogen. (a**)** Whole image with a scale bar of 20 μm. The surface and internal regions that are marked by the dotted line are enlarged in (b**)** and (c**)** with each scale bar of 1 μm.

nection of pores were observed at 30 min of etching. Figure 2c,d presents SEM images of the surface of the films treated with this etching process. Both the diameter and the interconnection of the crystalline network cylinder were similar to those before etching (see Figure 2a,b). This means that the amorphous component was selectively removed with 30 min of etching. Furthermore, the internal network structure is recognizable through the pores. The amorphous component must be continuous across the film thickness for such a deep etching. A pair of the remaining networks and pores for the etched sample corresponds to that of the initial bicontinuous cylinders of the crystalline and amorphous components before etching. This nanoporous structure extended over the whole film, which has a radius of 90 mm. ^{1}H NMR measurements showed that the disappearance of phenyl peak around 6−7 ppm after etching, indicating the complete removal of PS components.

To confirm the continuity of the pores across the film thickness, we observed the edge view of the etched film. A fresh edge was prepared by cleaving the etched film in liquid nitrogen. A similar cleavage observation was made for an internal characterization of nanoporous silica material.[6] Figure 3 presents a set of SEM images of the cleavage of the film

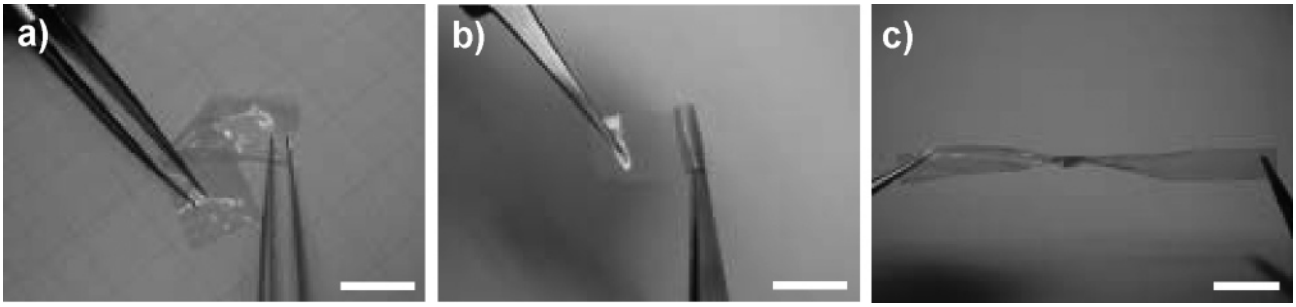

Figure 4. Photographs of the flexible nanoporous PE film prepared in this study on (a**)** bending, (b**)** rolling, and (c**)** knotting by tweezers with each scale bar of 10 mm.

etched for 30 min. The film thickness was 30 μm, the same as before the etching procedure. The crystalline network structure is clearly observable not only for the surface (b) but also for the internal regions (c) at the center of the film thickness. This means that fuming nitric acid etching was performed throughout the whole film. Also, this network morphology is consistent with the original etched film presented in Figure 2c,d. The unetched film was also cleft and its edge was observed at the same imaging magnitude for a comparison, but only the smooth morphology was obtained (not depicted here). Therefore, this network structure was formed by etching and not by cleaving.

The capability of this nanoporous structured film as a membrane material was evaluated by gas permeation measurements with argon and hydrogen gases. As a standard material, a commercial porous polyolefin membrane (U-Pore 3025, Ube) was adopted. This film has a comparable film thickness of 24 μm but a larger pore diameter exceeding 50 nm. Gas permeation analyses were performed using a homemade cell with pure argon and mixture of hydrogen/helium flows. The hydrogen gas permeation rate of this film was 2.5×10^7 mL mm m^{-2}. In contrast, our nanoporous structured film exhibits a hydrogen gas permeation rate of 3.5×10^7 mL mm m^{-2} under the same measurement conditions. It should be noted that the pore size of our film is almost half that of the commercial porous polyolefin membrane, but the gas permeation rate of our film is 1.4 times higher than that of the commercial membrane. This means that our film contains more developed pore networks across the film thickness.

Additionally, the pore size distribution of our etched film was evaluated by the BET method.[18] The mean value of the pore size was 30 nm, which is equivalent to the pore size observed in Figure 2. The average surface area of this nanoporous film was 17 m^2/g as obtained from the pore size distribution. This surface area is half of the 40 m^2/g calculated for the nanoporous ceramics prepared by Thomas et al.[2] However, it should be noted that such a comparable value was achieved even for flexible materials such as PE. As shown in Figure 4, the nanoporous PE film prepared in this study never breaks or tears by bending, rolling, and even knotting. Such superior characteristics should lead to a breakthrough in manufacturing the high-performance nanostructured membranes. For industrial application, the lower flexibility often causes breaking or tearing of the film, which would stop the continuous processing operation. In contrast, the resultant higher flexibility of our nanoporous film enables the efficient manufacturing.

Supporting Information Available: Details of experimental procedures. This material is available free of charge via the Internet at http://pubs.acs.org.

References and Notes

(1) Park, M.; Harrison, C.; Chaikin, P. M.; Register, R. A.; Adamson, D. H. *Science* **1997**, *276*, 1401.
(2) Chan, V. Z. H.; Hoffman, J.; Lee, V. Y.; Iatrou, H.; Avgeropoulos, A.; Hadjichristidis, N.; Miller, R. D.; Thomas, E. L. *Science* **1999**, *286*, 1716.
(3) Jeoung, E.; Galow, T. H.; Schotter, J.; Bal, M.; Ursache, A.; Tuominen, M. T.; Stafford, C. M.; Russell, T. P.; Rotello, V. M. *Langmuir* **2001**, *17*, 6396.
(4) Zalusky, A. S.; Olayo-Valles, R.; Taylor, C. J.; Hillmyer, M. A. *J. Am. Chem. Soc.* **2001**, *123*, 1519.
(5) Zalusky, A. S.; Olayo-Valles, R.; Wolf, J. H.; Hillmyer, M. A. *J. Am. Chem. Soc.* **2002**, *124*, 12761.
(6) Pai, R. A.; Humayun, R.; Schulberg, M. T.; Sengupta, A.; Sun, J.; Watkins, J. J. *Science* **2004**, *303*, 507.
(7) Jeong, U.; Kim, H.; Rodriguez, R. L.; Tsai, I. Y.; Stafford, C. M.; Kim, J. K.; Hawker, C. J.; Russell, T. P. *Adv. Mater.* **2002**, *14*, 274.
(8) Lei, L.; Yokoyama, H.; Nemoto, T.; Sugiyama, K. *Adv. Mater.* **2004**, *16*, 1226.
(9) Lei, L.; Yokoyama, H.; Nemoto, T.; Sugiyama, K. *Adv. Mater.* **2004**, *16*, 1542.
(10) Mao, H.; Hillmyer, M. A. *Macromolecules* **2005**, *38*, 4038.
(11) Olayo-Valles, R.; Guo, S.; Lund, M. S.; Leighton, C.; Hillmyer, M. A. *Macromolecules* **2005**, *38*, 10101.
(12) Hajduk, D. A.; Harper, P. E.: Gruner, S. M.; Honeker, C. C.; Kim, G.; Thomas, E. L.; Ferrers, L. J. *Macromolecules* **1994**, *27*, 4063.
(13) Uehara, H.; Nakae, M.; Kanamoto, T.; Ohtsu, O.; Sano, A.; Matsuura, K. *Polymer* **1998**, *39*, 6127.
(14) Phillips, R. A. *J. Polym. Sci., Polym. Phys. Ed.* **1998**, *36*, 495.
(15) Nakae, M.; Uehara, H.; Kanamoto, T.; Ohama, T.; Porter, R. S. *J. Polym. Sci., Polym. Phys. Ed.* **1999**, *37*, 1921.
(16) Cook, J. T. E.; Klein, P. G.; Ward, I. M.; Brain, A. A.; Farrar, D. F.; Rose, J. *Polymer* **2000**, *41*, 8615.
(17) Nakae, M.; Uehara, H.; Kanamoto, T.; Zachariades, A. E.; Porter, R. S. *Macromolecules* **2000**, *33*, 2632.
(18) Brunauer, S.; Emmett, P. H.; Teller, E. *J. Am. Chem. Soc.* **1938**, *60*, 309.

MA0601316